





RESEARCH PAPER

Direct measurement of hypoxia in a xenograft multiple myeloma model by optical-resolution photoacoustic microscopy

Toru Imai ^{a,*}, Barbara Muz ^{b,*}, Cheng-Hung Yeh^a, Junjie Yao^a, Ruiying Zhang ^a, Abdel Kareem Azab ^b, and Lihong Wang^a

^aDepartment of Biomedical Engineering, Washington University in St. Louis, St. Louis, MO, USA; ^bDepartment of Radiation Oncology, Cancer Biology Division, Washington University in St. Louis School of Medicine, St. Louis, MO, USA

ABSTRACT

Using photoacoustic microscopy (PAM), we evaluated non-invasively oxygenation and vascularization *in vivo* due to multiple myeloma (MM) progression. Mice injected with MM.1S-GFP were monitored with a fluorescence microscope for tumor progression. *In vivo* PAM of the cerebral bone marrow quantified the total oxygen saturation (sO_2). At 28 days after the MM cell injection, the total sO_2 had decreased by half in the developing tumor regions, while in the non-tumor regions it had decreased by 20% compared with the value at one day post MM injection. The blood vessel density was reduced by 35% in the developing tumor regions, while in the non-tumor regions it was reduced by 8% compared with the value at one day post MM injection. Hence, PAM corroborated the development of hypoxia due to MM progression and demonstrated decreased vascularization surrounding the tumor areas.

ARTICLE HISTORY

Received 9 November 2016
Accepted 18 December 2016

KEYWORDS

Angiogenesis; hypoxia; multiple myeloma; oxygenation; photoacoustic imaging

Introduction

Multiple myeloma (MM) is a plasma cell malignancy localized primarily in the bone marrow (BM).¹ Together with genetic and epigenetic changes, the BM microenvironment contributes to pathogenesis and facilitates MM progression. Novel therapies are being developed based on interrupting the interactions between MM cancer cells and the supportive BM microenvironment.^{1,2} The introduction of new therapeutics that include proteasome inhibitors has significantly improved the survival of MM patients; however, more than 90% of MM patients still relapse.²





In a growing tumor mass, cancer cell overgrowth is coupled with insufficient angiogenesis, which results in increasing regions of lowered oxygenation (hypoxia).^{3,4} Hypoxia is a potent factor activating various signaling pathways that contributes to an increased number of immature and leaky blood vessels, which further facilitate MM cell dissemination.⁴ An increase in vascular density in the BM, regulated at least in part by the hypoxia-inducible factor (HIF- α) pathway, was demonstrated in myeloma patients during monoclonal gammopathy of undetermined significance (MGUS) to MM progression.⁵

Hypoxia has been linked to a cancer stem cell-like phenotype maintaining a slow-cycling proliferation rate of cells,⁶ and also linked to treatment resistance in solid tumors as well as in MM.⁶ Thus, hypoxia is a negative prognostic factor for treatment efficacy and patient survival, demonstrating a potentially high therapeutic index.⁷ However, the evaluation of hypoxia in the tumor microenvironment largely relies on invasive methods, leading to an inevitable change of the targeting microenvironment. The current gold standard for measuring oxygen partial pressure in

solid tumors is a polarographic microelectrode.⁸ Other approaches to measure tumor oxygen levels include electron paramagnetic resonance oximetry, nuclear magnetic resonance spectroscopy, and positron emission tomography using nitroimidazole or ⁶⁴Cu-ATSM. One of the most common indirect measurements of oxygenation is performed only *ex vivo* by examining the expression of endogenous markers of hypoxia, such as HIF-1 α ,⁹ or by examining the cellular uptake of agents reduced in a hypoxic environment, such as pimonidazole.^{4,10}

Photoacoustic microscopy (PAM) is an emerging technique,^{11,12} widely applied in biomedical research ranging from the study of the mechanism of diseases, including a variety of cancers and stroke, to the study of functional connectivity of the brain.¹³ One notable advantage of PAM is the fact that hemoglobin is an endogenous absorption contrast; hence it enables label-free *in vivo* measurement of oxygen saturation (sO_2) of hemoglobin in red blood cells (RBCs) without disrupting the microenvironment. Furthermore, owing to its high sensitivity to optical absorption and the weak acoustic scattering in tissue, PAM possesses such a high imaging sensitivity that it enables monitoring a single flowing RBC with safe laser exposure.¹⁴ Thus, compared with other methods, PAM potentially provides a more accurate description of the oxygenation as well as vascularization of the microenvironment of the tumor.^{11,12}

In this study, using optical-resolution photoacoustic microscopy (OR-PAM),¹⁵ we measured the spatial distribution of sO_2 of blood vessels in the BM in the mouse skull. With its high spatial resolution of a few micrometers, OR-PAM can precisely image the sO_2 distribution in this microenvironment. We also

CONTACT Abdel Kareem Azab  kareem.azab@wustl.edu  Department of Radiation Oncology, Cancer Biology Division, Washington University in St. Louis School of Medicine, 4511 Forest Park Ave., Room 3103, St. Louis, MO 63108, USA; Lihong Wang  lhwang@wustl.edu, lhwang@biomed.wustl.edu  Department of Biomedical Engineering, Washington University in St. Louis One Brookings Drive, Campus Box 1097, St. Louis, MO 63130, USA.

*These authors contributed equally to this work.

monitored the sO_2 changes induced by MM cell progression in the BM.

Results

In order to directly monitor and image the oxygenation level and blood vessel density during MM progression in the BM *in vivo*, we used an OR-PAM imaging system demonstrated in a schematic diagram in Fig. 1A. We performed OR-PAM within the frontal bone of the skull in MM-bearing SCID mice (Fig. 1B), which allowed to visualize and measure oxygen saturation of hemoglobin in RBCs in the BM with minimal invasiveness to the tumor microenvironment. Fig. 2A shows fluorescence microscope images of the MM tumor development in the BM of the skull after injection of MM1s-GFP cells, as well as PAM of the sO_2 and the vascularization in the normal and tumor BM areas as shown in Fig. 2B. Quantification of the fluorescence images shows that the tumor size within the tumor regions increased over 4 weeks after the cell injection (Fig. 2C).

The total sO_2 levels in normal and tumor areas at 14 and 28 days post cell injection were measured by PAM. It was found that the total sO_2 levels decreased over time, while the level of total sO_2 in adjacent normal BM areas did not change over time. At day 28, the total sO_2 level in the developing tumor regions decreased to an average of $50\% \pm 15\%$ of the value at one day post MM injection, while in the non-tumor regions the total sO_2 level decreased to $88\% \pm 16\%$ (Fig. 2Di). The total sO_2 level was shown to be inversely correlated with the tumor burden (Fig. 2Dii). Additionally, at day 28, the averaged sO_2 level in the developing tumor regions decreased to an average

of $87\% \pm 8\%$ of the value at one day post MM injection, while in the non-tumor regions the averaged sO_2 level slightly increased to $102\% \pm 7\%$.

Moreover, we quantified the vascularization (vessel density) in normal and tumor areas of the BM after the injection of MM cells. A significant reduction of blood vessel density was observed in the tumor region, while the level of vascularization did not change in normal BM areas. The blood vessel density in the developing tumor regions decreased to an average of $65\% \pm 12\%$ of the value at one day post MM injection, while in the non-tumor regions, it decreased to $92\% \pm 15\%$ (Fig. 2Ei). The level of vascular density was shown to be inversely correlated with the tumor burden (Fig. 2Eii).

Discussion

Based on our results, we obtained clear evidence that the total sO_2 levels in the MM cell proliferation regions were significantly lower than in the normal (non-tumor affected) regions. The localized and gradual decrease of the total sO_2 level in the tumor regions is considered to indicate a corresponding decrease in the total amount of oxygen, which in turn is considered to naturally induce hypoxia in the region. Therefore, our results suggest that the hypoxia was developed by the proliferation of the MM cells, which is in agreement with previously published studies.^{4,6} Unlike other invasive techniques, PAM provided real-time visual evidence for the development of hypoxic and low vascularization regions due to tumor development, without disrupting the microenvironment. Based on our results, the blood vessel density in the tumor regions decreased

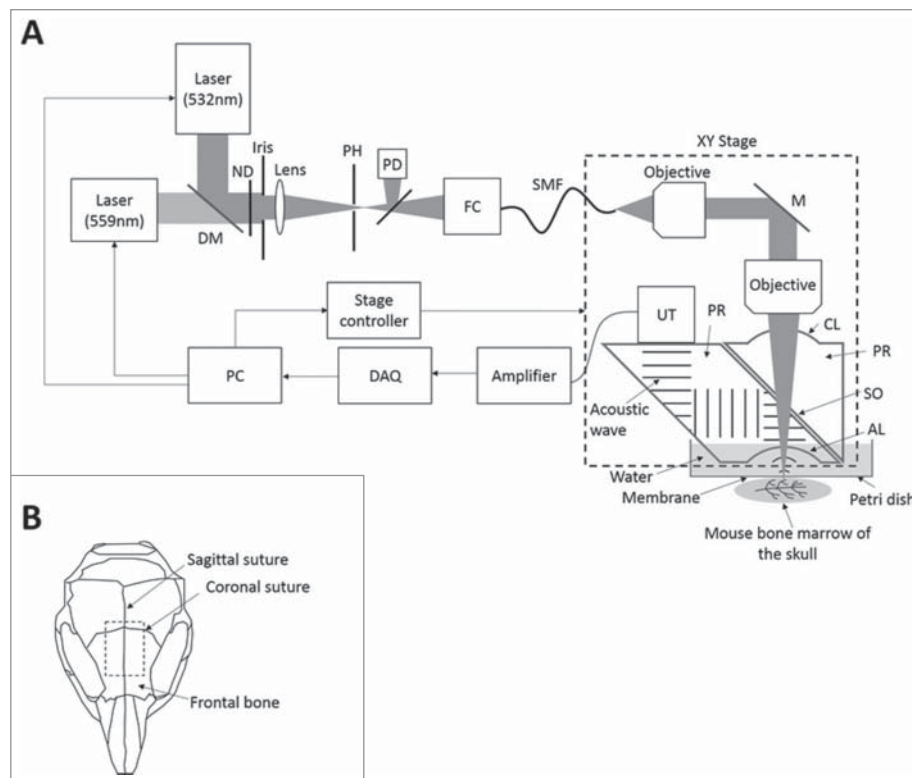


Figure 1. Optical-resolution photoacoustic microscopy (OR-PAM) for *in vivo* imaging of oxygenation and vascularization in the bone marrow. (A) Schematic diagram of the OR-PAM imaging system. AL, acoustic lens; CL, correction lens; DAQ, data acquisition; DM, dichroic mirror; FC, fiber coupler; M, mirror; ND, neutral density filter; PD, photodiode; PH, pinhole; PR, prism; SMF, single-mode fiber; SO, silicone oil; UT, ultrasonic transducer. (B) Imaging regions in the mouse skull.

as the tumor developed. This fact indicates a decrease of the blood flow rate of these regions, unless the blood velocity increased to offset the effect of the reduction of the blood vessel density, which is unlikely. Furthermore, the fact that the averaged sO_2 level decreased more in the tumor developing regions indicates a decrease in the difference between the arterial and venous oxygen concentration, assuming the oxygen extraction rate remained at the same level. Therefore, our results reasonably indicate a more hypoxic condition in the tumor developing regions, which is also predicted by the general formula describing oxygen consumption in tissue. However, a direct correlation between the hypoxic condition in the microenvironment, the reduction in the total or averaged sO_2 level and blood vessel density needs to be established.

In this study, we did not clarify the reason for the slight reductions of the total sO_2 level and blood vessel density in the normal region, which are thought to be caused by the surgical operations in the experiment. Specifically, the relatively long-term monitoring or/and the frequent incision of the scalp of the mouse for the imaging window could induce the slight physiologic change in the blood vessels in the BM. However, the results for the total sO_2 level and blood vessel density in the tumor region also included the same effect as the normal region, so we believe our conclusions were not affected. To prevent the undesirable effect of repeated incision, we could monitor each mouse at only a single but different time point.

We also found that the vascularization in the tumor mass decreased 4 weeks post MM cell injection, which conflicts with the current state of knowledge. Angiogenesis, new blood vessel formation from existing vasculature, is one of the best-described cause-effect consequences of tumor hypoxia, and plays a pivotal role in tumor progression in cancer.¹⁶ It was previously reported that vascular density in the BM increased in myeloma patients during MGUS to MM progression.¹⁷ Furthermore, monitoring the microvessel density in the BM demonstrated that high-grade angiogenesis at diagnosis was predictive of poorer response to high-dose induction therapy in newly diagnosed patients, and contributed to poor prognosis in myeloma patients.¹⁸ The differences between our findings and those elsewhere in the literature need to be further explored.

For future work, by taking advantage of the desirable characteristics of PAM, namely, its minimal invasiveness, high spatial resolution, high speed, high sensitivity, and functional imaging capability, we can naturally extend it to evaluating the efficacy of therapeutic drugs targeting MM cells. PAM will give us a more direct indication of the relationship between the effectiveness of the drugs and hypoxia.

Materials and methods

MM mouse model

Severe combined immune deficiency (SCID) mice (female, 8-weeks old) were obtained from Envigo. Approval for these studies was obtained from the Animal Studies Committee at Washington University in St. Louis. The experiments were executed in compliance with institutional guidelines and regulations. MM.1S used in this manuscript was freshly obtained from American Type Culture Collection (ATCC) and characterized by ATCC based on the karyotype and expression of

cluster of differentiation (CD) markers, receptors and light chain immunoglobulin. MM.1S were genetically engineered to express green fluorescent protein (GFP) as described previously.¹⁶ Cells were cultured in RPMI-1640 medium (Corning CellGro), supplemented with 10% fetal bovine serum (Life Technologies/Gibco), 2 mmol/l of L-glutamine, 100 U/ml of penicillin, and 100 μ g/ml of streptomycin (CellGro) at 37°C and 5% CO_2 in a humidified tissue culture incubator (NuAire). The cells are routinely tested for mycoplasma using the Plasmotest kit (InvivoGen) and according to the manufacturer's protocol. For the study, 2 mice were injected intravenously (IV) via the tail vein with 4×10^6 MM.1S-GFP per mouse. The injected MM.1S dominantly home to the bone marrow in the whole body, including the skull bone marrow, as described in the previous research.⁴

Imaging of MM cells in vivo

To monitor the tumor progression, the mouse brain was imaged with a wide field fluorescence microscope (FluoView FV1000, Olympus) using 4X or 10X objectives. To measure the fluorescence of GFP tagged to MM cells, a standard filter set was used (NIBA3: excitation filter 470–495 nm, emission filter 510–550 nm). The imaging region was within the frontal bone, where most of the skull bone marrow is located (Fig. 1B).^{4,17} We monitored the tumor progression by measuring at several time points: 1, 14 and 28 days after MM.1S-GFP cell injection. During the imaging, the mice were under inhalational anesthesia with 1.5% isoflurane (Isothesia). The scalp of the mouse was surgically incised to form a flap through which the skull was imaged, but the skull remained intact. After each monitoring, the flap was stitched closed.

Photoacoustic imaging

To measure the photoacoustic signal and the sO_2 level of RBCs in the blood vessels of the mouse brain, we used our previously developed OR-PAM (Fig. 1A).¹⁵ The system consisted of 2 diode-pumped solid-state lasers for photoacoustic excitation with 2 different wavelengths (InnoSlab, Edgewave, for 559 nm, and SPOT-10–200–532, Elfolight, for 532 nm). The 2 laser beams with different wavelengths were combined through a dichroic mirror, whose transmission and reflection rates were selected so that 559 nm light passed through and 532 nm light was reflected. During imaging, the 2 laser beams sequentially irradiated the target. The repetition rate of each laser was 10 kHz. To detect the photoacoustic signal, the system used an ultrasonic transducer with a 50 MHz central frequency (V214-BB-RM, Olympus). To acquire 2-dimensional images, the system used 2 motorized translational stages, which enabled 2-dimensional raster scanning. The step sizes for imaging were 2.5 μ m along the fast axis and 5 μ m along the slow axis, and imaging a 4 mm by 6 mm area took around 10 minutes. The lateral resolution of this system could reach 2.6 μ m (full width at half maximum) when a smaller step size was used.¹⁵

sO_2 imaging in vivo

We acquired the photoacoustic signal excited at the 2 different wavelengths to calculate the sO_2 level at each pixel.¹⁵

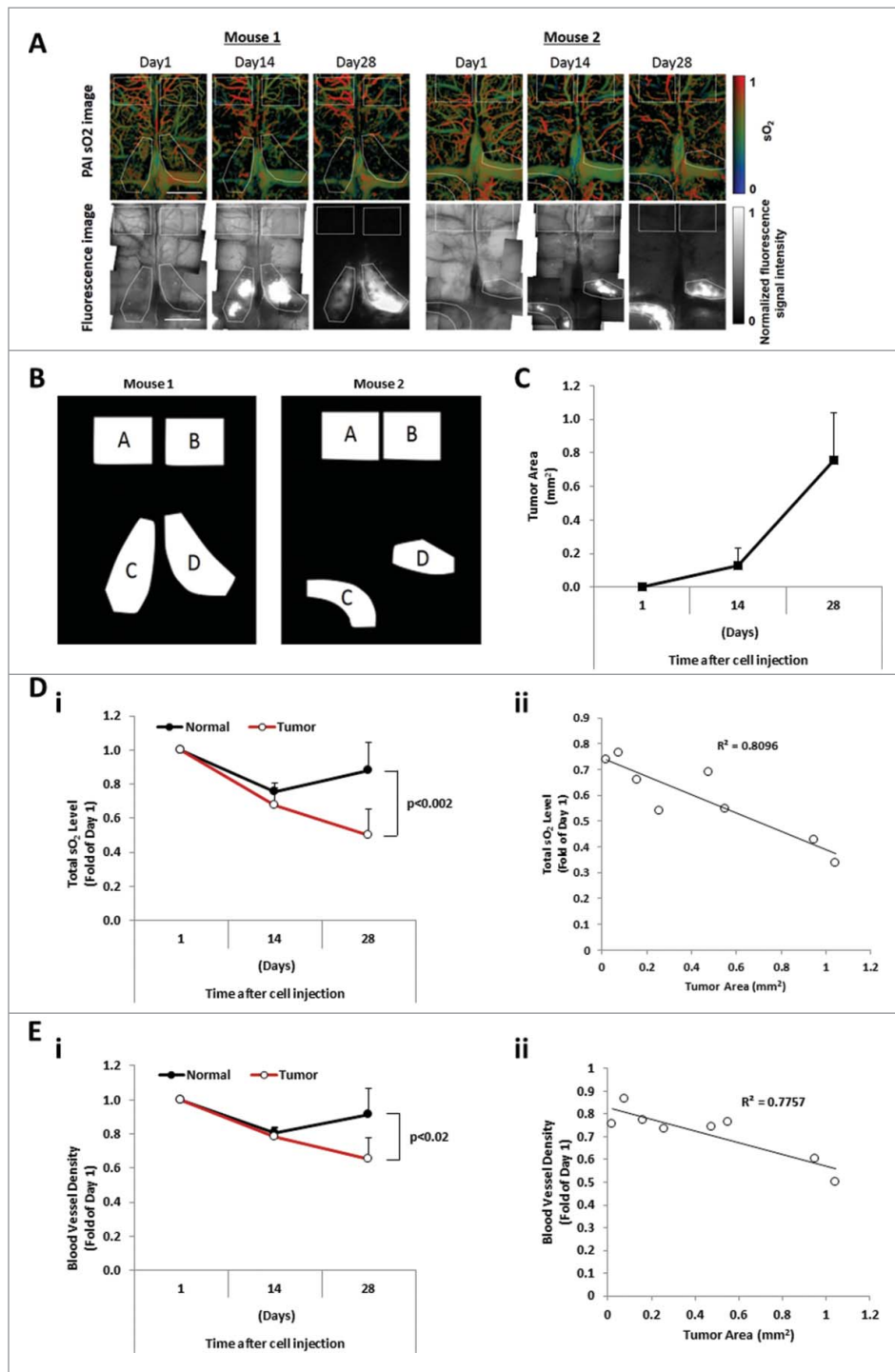


Figure 2. The sO₂ level and blood vessel density are inversely correlated with the tumor burden. (A) Images of sO₂ levels acquired by OR-PAM and the corresponding fluorescence microscopy images. The mouse brain was imaged at Day 1, Day 14, and Day 28 after intravenous injection of MM cells. Scale bars: 1 mm. (B) Designated regions of interest (ROI) of mouse 1 and mouse 2 used for analysis denoted as normal areas, regions A and B, and tumor areas, regions C and D. (C) Tumor progression evaluated as the tumor area (mm²) measured at Days 1, 14, and 28 post MM cell injection (mean ± SD), n = 4. (Di) Comparison of average relative total sO₂ level between tumor and normal regions over the course of 4 weeks and normalized to Day 1 post MM injection (mean ± SD), n = 4. (Dii) Correlation between the oxygenation (total sO₂) and the tumor area (mm²) with correlation coefficient $R^2 = 0.8096$. (Ei) Comparison of average blood vessel density between tumor and normal regions over the course of 4 weeks and normalized to Day 1 post MM injection (mean ± SD), n = 4. (Eii) Correlation between the blood vessel density and the tumor area (mm²) shows a correlation coefficient $R^2 = 0.7757$.

OR-PAM imaging was performed on the same day and over the same imaging region as for the fluorescence microscope. As during imaging by the fluorescence microscope, the mice were under inhalational anesthesia with isoflurane during OR-PAM imaging. Also as before, the scalp of the mouse was retracted, but its skull remained intact.

Analysis of tumor progression, oxygenation, and blood vessel density

To evaluate tumor progression and oxygenation based on the images acquired by the fluorescence microscope and OR-PAM system, we defined 2 comparable regions of interest (ROI) for

quantification: One was the tumor region, which included the area where the tumor had developed most significantly, based on the GFP signal intensity at 28 days after MM cell injection (regions C and D in Fig. 2A). The other was a normal region, which was designated as the area located as far as possible from all tumor regions within the field of view (regions A and B in Fig. 2A). In all normal regions, we confirmed that much weaker fluorescence signals were detected in the normal regions. For each mouse, we selected 2 tumor regions and 2 corresponding normal regions (Fig. 2B). To evaluate the tumor burden, we calculated the area of the tumor within the tumor regions at different time points. The area of the tumor within tumor regions was defined as the group of pixels of the fluorescence image whose brightness was higher than twice the average brightness of the normal regions. After co-registering the fluorescence and photoacoustic images based on the structure of blood vessels, we also evaluated the total sO_2 level, the averaged sO_2 level, and blood vessel density in the defined ROIs. The total sO_2 level within each ROI was calculated as the summation of the sO_2 levels of all pixels of the imaged blood vessels. The averaged sO_2 level within the ROI was calculated as the average of the sO_2 levels of all pixels of the imaged blood vessels. The blood vessel density was calculated as the ratio of the number of pixels of the imaged blood vessels to that of each ROI.

Statistical analysis

The data were expressed as mean \pm standard deviation. Results were analyzed using Two Way ANOVA for statistical significance and were considered significantly different for a P value less than 0.05.

Disclosure of potential conflicts of interest

L.V.W. has financial interests in Microphotoacoustics, Inc., which; however, did not support this work. A.K.A. reports receiving research support from Verastem, Selexys, Karyopharm, Cell Works, Cleave Bioscience, Glycomimetics, Abbvie and Vasculox; and is the founder and owner of Targeted Therapeutics LLC and Cellatrix LLC, which; however, did not support this work. All other authors state no conflicts of interest.

Acknowledgement

The authors appreciate the close reading of the manuscript by Prof. James Ballard. We also thank Lei Li for helpful discussions. This work was sponsored by National Institutes of Health Grants R01 CA186567 (NIH Director's Transformative Research Award), U01 NS090579 (BRAIN Initiative), and R01 CA159959, all to L.V.W.

A.K.A. is supported by grants from National Institutes of Health under Award Number U54CA199092, the Multiple Myeloma Research Foundation, the International Waldenström Macroglobulinemia Foundation and Bear Cub Award (Skandalaris Center at Washington University in St. Louis).

ORCID

Toru Imai  <http://orcid.org/0000-0002-9497-8549>
 Barbara Muz  <http://orcid.org/0000-0003-4125-4624>
 Ruiying Zhang  <http://orcid.org/0000-0002-0092-0814>
 Abdel Kareem Azab  <http://orcid.org/0000-0002-6371-2780>

References

- Kyle RA, Rajkumar SV. Multiple myeloma. *Blood* 2008; 111:2962-72; PMID:18332230; <http://dx.doi.org/10.1182/blood-2007-10-078022>

- Nair RR, Gebhard AW, Emmons MF, Hazlehurst LA. Emerging strategies for targeting cell adhesion in multiple myeloma. *Adv Pharmacol* 2012; 65:143-89; PMID:22959026; <http://dx.doi.org/10.1016/B978-0-12-397927-8.00006-3>
- Asosingh K, De Raeve H, de Ridder M, Storme GA, Willems A, Van Riet I, Van Camp B, Vanderkerken K. Role of the hypoxic bone marrow microenvironment in 5T2MM murine myeloma tumor progression. *Haematologica* 2005; 90:810-7; PMID:15951294
- Azab AK, Hu J, Quang P, Azab F, Pitsillides C, Awwad R, Thompson B, Maiso P, Sun JD, Hart CP, et al. Hypoxia promotes dissemination of multiple myeloma through acquisition of epithelial to mesenchymal transition-like features. *Blood* 2012; 119:5782-94; PMID:22394600; <http://dx.doi.org/10.1182/blood-2011-09-380410>
- Rajkumar SV, Mesa RA, Fonseca R, Schroeder G, Plevak MF, Dispenzieri A, Lacy MQ, Lust JA, Witzig TE, Gertz MA, et al. Bone marrow angiogenesis in 400 patients with monoclonal gammopathy of undetermined significance, multiple myeloma, and primary amyloidosis. *Clin Cancer Res* 2002; 8:2210-6; PMID:12114422
- Muz B, de la Puente P, Azab F, Luderer M, Azab AK. Hypoxia promotes stem cell-like phenotype in multiple myeloma cells. *Blood Cancer J* 2014; 4:e262; PMID:25479569; <http://dx.doi.org/10.1038/bcj.2014.82>
- Martin SK, Diamond P, Gronthos S, Peet DJ, Zannettino AC. The emerging role of hypoxia, HIF-1 and HIF-2 in multiple myeloma. *Leukemia* 2011; 25:1533-42; PMID:21637285; <http://dx.doi.org/10.1038/leu.2011.122>
- Milosevic M, Fyles A, Hedley D, Hill R. The human tumor microenvironment: invasive (needle) measurement of oxygen and interstitial fluid pressure. *Semin Radiat Oncol* 2004; 14:249-58; PMID:15254868; <http://dx.doi.org/10.1016/j.semradonc.2004.04.006>
- Koukourakis MI, Giatromanolaki A, Polychronidis A, Simopoulos C, Gatter KC, Harris AL, Sivridis E. Endogenous markers of hypoxia/anaerobic metabolism and anemia in primary colorectal cancer. *Cancer Sci* 2006; 97:582-8; PMID:16827797; <http://dx.doi.org/10.1111/j.1349-7006.2006.00220.x>
- Bussink J, Kaanders JH, van der Kogel AJ. Tumor hypoxia at the micro-regional level: clinical relevance and predictive value of exogenous and endogenous hypoxic cell markers. *Radiother Oncol* 2003; 67:3-15; PMID:12758235; [http://dx.doi.org/10.1016/S0167-8140\(03\)00011-2](http://dx.doi.org/10.1016/S0167-8140(03)00011-2)
- Wang LV, Hu S. Photoacoustic tomography: *in vivo* imaging from organelles to organs. *Science* 2012; 335:1458-62; PMID:22442475; <http://dx.doi.org/10.1126/science.1216210>
- Yao J, Wang LV. Photoacoustic microscopy. *Laser Photon Rev* 2013; 7:5; PMID:24416085; <http://dx.doi.org/10.1002/lpor.201200060>
- Yao J, Wang LV. Photoacoustic brain imaging: from microscopic to macroscopic scales. *Neurophotonics* 2014; 1:1; PMID:25401121; <http://dx.doi.org/10.1117/1.NPH.1.1.011003>
- Wang L, Maslov K, Wang LV. Single-cell label-free photoacoustic flowography *in vivo*. *Proc Natl Acad Sci U S A* 2013; 110:5759-64; PMID:23536296; <http://dx.doi.org/10.1073/pnas.1215578110>
- Hu S, Maslov K, Wang LV. Second-generation optical-resolution photoacoustic microscopy with improved sensitivity and speed. *Opt Lett* 2011; 36:1134-6; PMID:21479007; <http://dx.doi.org/10.1364/OL.36.001134>
- Folkman J. Tumor angiogenesis: therapeutic implications. *N Engl J Med* 1971; 285:1182-6; PMID:4938153; <http://dx.doi.org/10.1056/NEJM197108122850711>
- Kumar S, Witzig TE, Timm M, Haug J, Wellik L, Kimlinger TK, Greipp PR, Rajkumar SV. Bone marrow angiogenic ability and expression of angiogenic cytokines in myeloma: evidence favoring loss of marrow angiogenesis inhibitory activity with disease progression. *Blood* 2004; 104:1159-65; PMID:15130943; <http://dx.doi.org/10.1182/blood-2003-11-3811>
- Kumar S, Gertz MA, Dispenzieri A, Lacy MQ, Wellik LA, Fonseca R, Lust JA, Witzig TE, Kyle RA, Greipp PR, et al. Prognostic value of bone marrow angiogenesis in patients with multiple myeloma undergoing high-dose therapy. *Bone Marrow Transplant* 2004; 34:235-9; PMID:15170170; <http://dx.doi.org/10.1038/sj.bmt.1704555>